

CONTROLLED LONGITUDINAL EMITTANCE BLOW-UP FOR HIGH INTENSITY BEAMS IN THE CERN SPS

D. Quartullo*, H. Damerou, I. Karpov, G. Papotti,
E. Shaposhnikova, C. Zisou, CERN, Meyrin, Switzerland

Abstract

Controlled longitudinal emittance blow-up will be required to longitudinally stabilise the beams for the High-Luminosity LHC in the SPS. Bandwidth-limited noise is injected at synchrotron frequency sidebands of the RF voltage of the main accelerating system through the beam phase loop. The setup of the blow-up parameters is complicated by bunch-by-bunch differences in their phase, shape, and intensity, as well as by the interplay with the fourth harmonic Landau RF system and transient beam loading in the main RF system. During previous runs, an optimisation of the blow-up had to be repeated manually at every intensity step up, requiring hours of precious machine time. With the higher beam intensity, the difficulties will be exacerbated, with bunch-by-bunch differences becoming even more important. We look at the extent of the impact of intensity effects on the controlled longitudinal blow-up by means of macro-particle tracking, as well as analytical calculations, and we derive criteria for quantifying its effectiveness. These studies are relevant to identify the parameters and observables which become key to the operational setup and exploitation of the blow-up.

INTRODUCTION

The “High Luminosity LHC” (HL-LHC) proton beams in the SPS will require stabilization in the longitudinal plane [1–3]. A fourth harmonic 800 MHz RF system in combination with the 200 MHz accelerating one will increase the synchrotron frequency spread inside the bunch enhancing Landau damping [4], whereas controlled blow-up will increase the bunch longitudinal emittance in a controlled way [5]. Both methods will be required to cope with coupled-bunch instabilities along the ramp and at flat-top.

Controlled emittance blow-up is achieved in the SPS by injecting bandwidth-limited phase noise into the phase-loop of the main RF system [6], as done also in the CERN PSB and LHC [7–10]. Phase noise should diffuse just the particles situated in the bunch core, since affecting the tails could lead to particle losses. Emittance blow-up should occur along the SPS ramp, so that particles driven out of the buckets are lost in the SPS, and are not transferred to the LHC.

The noise-generation algorithm produces digital, band-limited phase noise samples. Since the frequency band should cover the synchrotron frequencies of the particles situated in the bunch core, it must follow the changes of synchrotron frequencies during the ramp. The noise generation algorithm receives the required frequency band as input and produces phase noise with the desired spectral properties.

* danilo.quartullo@cern.ch

One main remaining issue is the determination of the optimal frequency band. A dedicated algorithm has been developed for this purpose. The frequency band is obtained by designing the emittance increase during blow-up and by making use of accurately computed synchrotron-frequency distributions, which include collective effects.

Longitudinal beam dynamics simulations of the SPS cycle are important to validate the effectiveness of the computed frequency bands. One batch of 72 bunches was tracked including the full SPS impedance model, beam loops and emittance blow-up. Simulations were then compared with beam measurements during the SPS cycle. The computed frequency bands provided useful input to set the phase-noise parameters with beam.

In this paper we describe the implementation of emittance blow-up in operation. Then, the procedure for the determination of the phase-noise frequency band is explained in detail. Results from beam dynamics simulations are reported and compared with first beam measurements.

IMPLEMENTATION OF THE PHASE-NOISE ALGORITHM

The HL-LHC beam requirements drove the LHC Injector Upgrade Project [11], which, at the SPS, foresaw a complete renovation of the RF system, including a rearrangement of the 200 MHz accelerating structures, and a redesign of the Low Level controls (LLRF, [12]), based on the MicroTCA platform, and featuring a restructuring of the beam control loops. The controlled emittance blow-up was operational for LHC-type beams in previous runs (2010-2018) [6], and had to be re-implemented in the new LLRF system. The addition of the noise in the phase loop is now done in the new, digital LLRF, but the previous algorithm for the preparation of the noise pattern and the high level controls are maintained.

The noise algorithm [13] creates an excitation spectrum that follows the varying frequency spectrum during the energy ramp, and that is band-limited, with very low leakage. The noise frequency bands are calculated in the SPS high level controls (LHC Software Architecture, LSA), and sent to the C++ code that prepares the noise pattern. The central synchrotron frequency f_{s0} in double-RF system without intensity effects is automatically calculated in LSA. The low and high band-limits are obtained by multiplying the calculated f_{s0} by two knobs, so to scale them easily.

DETERMINATION OF THE PHASE-NOISE FREQUENCY BAND

A first algorithm for the determination of the frequency band has been developed. It does not require particle track-

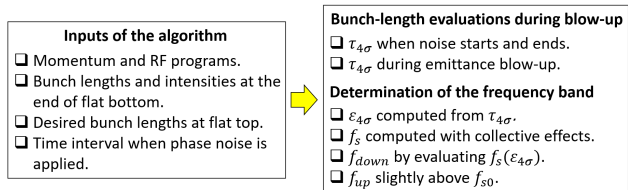


Figure 1: Scheme of the algorithm for the determination of the phase-noise frequency band.

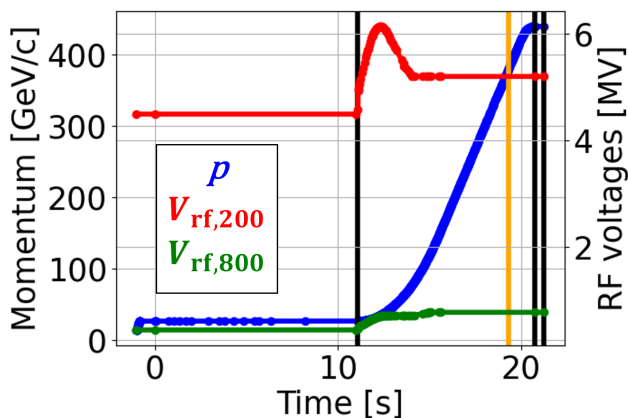


Figure 2: Momentum program (blue), main (red) and fourth (green) harmonic RF programs for the SPS HiRadMat cycle during scrubbing in August 2021. The black lines mark the start of the ramp (11.10 s), the end of the ramp (20.77 s) and the extraction time (21.27 s). The orange line corresponds to the momentum of 380 GeV/c.

ing, but it exploits the generation of distributions matched to the RF bucket with intensity effects to evaluate the bunch lengths and emittances during the blow-up. A scheme of the algorithm structure is shown in Fig. 1.

Inputs of the Algorithm

The algorithm takes as inputs the momentum and RF programs, the bunch lengths and intensities at the end of the flat-bottom, the desired bunch lengths at flat-top after emittance blow-up, as well as the cycle times when phase noise should start and end.

Figure 2 shows the momentum program of the SPS HiRadMat cycle, together with the programs of the main and fourth harmonic RF systems during scrubbing (with limited RF voltage) in August 2021. The HiRadMat cycle accelerates up to 4 batches of 72 bunches from flat bottom (26 GeV/c) to flat-top (440 GeV/c). Bunch rotation is applied in the CERN PS at flat-top in order to reduce the length of the bunches and make them fit into the SPS RF buckets.

The program of the main RF system in Fig. 2 provides 4.5 MV and 5.2 MV at flat bottom and top, respectively. The voltage bump allows a constant bucket area in that time interval. The fourth harmonic RF system increases the synchrotron frequency spread inside the bunch, enhancing Landau damping. In Fig. 2, the voltage ratio between the two RF systems is 10% at flat bottom, it increases linearly during

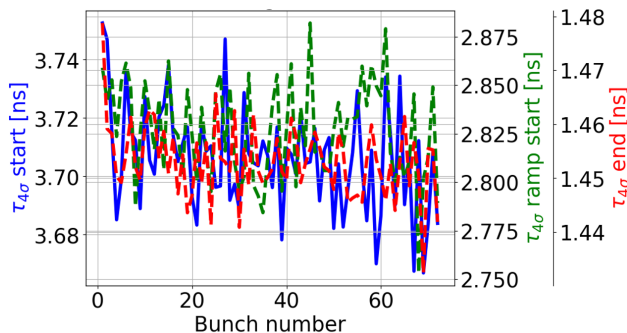


Figure 3: Simulated bunch lengths along the batch at SPS injection (blue), after 0.5 s of flat bottom (green) and at extraction (red). The BLoND simulations used the programs shown in Fig. 2 and started from realistic rotated PS bunch distributions. Emittance blow-up was not applied.

the first part of acceleration and remains at 15% until extraction. The phase between the RF systems is programmed for bunch-shortening mode (BSM) [4].

The bunch intensities and lengths at the end of the flat-bottom were obtained by performing macro-particle simulations. One batch of 72 bunches was simulated for 0.5 s at flat bottom, using the CERN BLoND code [14]. Simulations included the full SPS impedance model and started from realistic bunch distributions, with an intensity of $1.2 \cdot 10^{11}$ ppb and which were obtained by performing simulations of bunch rotation at PS flat-top with collective effects.

The effect of the One Turn Delay Feedback (OTFB) for beam loading compensation was added in simulations by reducing the shunt impedances of the RF fundamental modes by -26 dB. An accurate model of the beam-based phase, synchro and frequency loops was used in simulations.

The obtained bunch lengths at injection (blue) and after 0.5 s of flat bottom (green) are reported in Fig. 3, where $\tau_4 = \sqrt{2} \tau_{FWHM} / \sqrt{\ln 2}$ is the convention used in the SPS to compute bunch lengths, τ_{FWHM} being the Full Width at Half Maximum of the bunch profile. The bunch lengths at injection in Fig. 3 are within 3.71 ± 0.04 ns, whereas those at the ramp start are $\tau_{4,rs} = 2.83 \pm 0.08$ ns.

The desired bunch length $\tau_{4,d}$ at extraction after having applied emittance blow-up should satisfy the cycle-dependent beam requirements and should be large enough to ensure beam stability. Typical values of desired $\tau_{4,d}$ are between 1.6 ns and 2.0 ns. Without emittance blow-up and for low intensities, the bunch lengths $\tau_{4,ex}$ at extraction vary usually between 1.45 ns and 1.65 ns (see e.g. Fig. 3, red). Above $1.6 \cdot 10^{11}$ ppb, a single LHC batch without blow-up is expected to become unstable during the SPS ramp.

The last input parameter for the algorithm is the time interval when phase noise is applied. Concerning the HiRadMat cycle, the starting time of phase noise was set to $t_s = 15$ s, when the bucket area starts to increase, which reduces particle losses when phase noise is applied.

In general, long time intervals with phase noise are desirable, since they allow more possibilities in the design

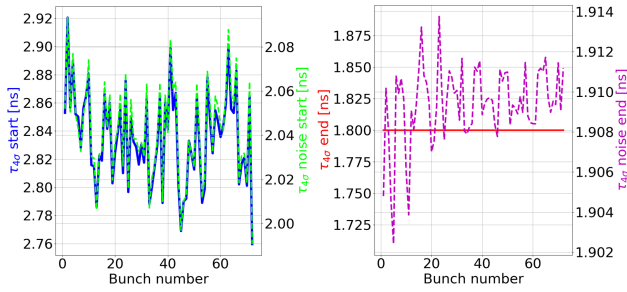


Figure 4: Bunch lengths along the batch at cycle times t_s (green) and t_e (magenta), obtained from the algorithm for frequency band determination using the momentum and voltage programs shown in Fig. 2. The bunch lengths at the end of the flat-bottom (blue) and the desired bunch lengths at extraction (red) are input parameters to the algorithm.

of the blow-up manipulation and allow also a slower, and therefore more controlled, bunch-length increase. However, emittance blow-up at the flat-top could lead to transfer to the LHC of particles pushed outside of the SPS buckets by the phase noise. In addition, a transverse scraping starting at 380 GeV/c is foreseen for the HL-LHC beams and, to limit losses, phase noise should stop before this scraping begins. Since a momentum of 380 GeV/c corresponds to the cycle time of 19.3 s (Fig. 2, orange line), the end of phase noise was set to $t_e = 19$ s, leaving 300 ms of margin.

Bunch-length Evaluations During the Blow-up

The first step performed by the algorithm is to estimate the bunch lengths at t_s and t_e . Since the different $\tau_{4,rs}$ at ramp start are known, we can generate a matched distribution for each bunch and compute the corresponding full emittance ϵ_f . Assuming that ϵ_f is preserved until phase noise starts, the ϵ_f values are used to generate matched distributions and to compute the bunch lengths at t_s . This procedure of double matching is also applied to find the bunch lengths at t_e . Then, for each bunch, the computed $\tau_{4,s}$ and $\tau_{4,e}$ are linearly interpolated to obtain the design τ_4 during the blow-up.

Figure 4 shows an example of bunch lengths at t_s and t_e computed with the algorithm, assuming $\tau_{4,d} = 1.8$ ns. The variations of τ_4 along the batch are similar at times t_{rs} and t_s . The values are $\tau_{4,rs} = 2.84 \pm 0.08$ ns, $\tau_{4,s} = 2.04 \pm 0.05$ ns and $\tau_{4,e} = 1.91 \pm 0.01$ ns.

The generated bunch distributions are binomial. Since it is not easy to foresee the profile shapes at t_s and t_e , it is important that the bunch lengths at these times do not significantly depend on the exponent μ of the binomial distribution. This occurs for a relatively large range of μ values, as shown in the example in Fig. 5, where the FWHM bunch lengths at t_e differ by just 1% when μ varies between 0.5 and 2.5.

Determination of the Frequency Bands

At a given time between t_s and t_e , and for each bunch, a matched distribution with the interpolated τ_4 is generated. The emittance ϵ_4 corresponding to τ_4 is then computed.

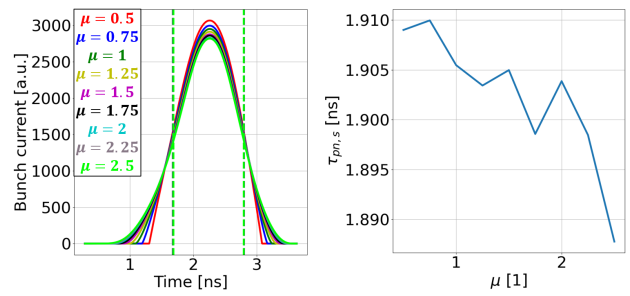


Figure 5: Left: bunch profiles obtained from binomial distributions matched in phase space at time t_e with different μ . The profiles refer to the first bunch of the batch, assuming $\tau_{4,d} = 1.8$ ns. The dashed lines determine τ_{FWHM} . Right: τ_{FWHM} corresponding to the profiles on the left.

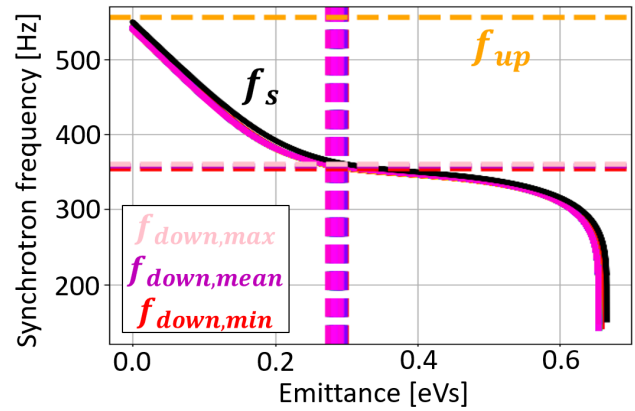


Figure 6: Synchrotron frequency distributions at t_s without (black) and with (other colours) collective effects for 72 bunches with intensity $1.2 \cdot 10^{11}$ ppb. The peak voltages of the main and fourth harmonic RF systems are 5.2 MV and 0.78 MV respectively, the phase is programmed for BSM. The vertical lines mark the ϵ_4 emittances of the 72 bunches (Fig. 7, left). The horizontal lines indicate the maximum, mean, minimum of the f_{down} values (Fig. 7, right), and the frequency-band upper limit, which is set slightly above f_{s0} .

Thereafter, for each bunch, the synchrotron frequency distribution including collective effects is evaluated (Fig. 6), this allows to determine f_{down} (Fig. 7, right) as the frequency corresponding to ϵ_4 (Fig. 7, left). In general, larger emittances correspond to lower f_{down} values, although the increase of f_{down} along the first 20 bunches in Fig. 7 (right) is mostly due to collective effects which change the shapes of the synchrotron frequency distributions.

Since only one value of f_{down} can be chosen for all the bunches at a given time, the maximum, mean and minimum of the f_{down} values were considered, as shown in Figs. 6 and 7 (right). The minimum f_{down} targets at least ϵ_4 for each bunch. If the target emittance is larger than ϵ_4 , then bunches could be affected also in the tails, especially when ϵ_4 is close to the inflection point of the synchrotron frequency distribution (see e.g. Fig. 6). Selecting the maximum f_{down} allows targeting at most ϵ_4 for each bunch, with some bunches not

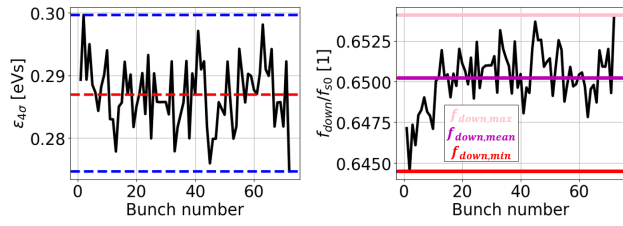


Figure 7: Emittance ϵ_4 (left) and normalized f_{down} (right) along the batch at time t_s . The emittances are obtained from the bunch lengths at t_s (Fig. 4, left, green line).

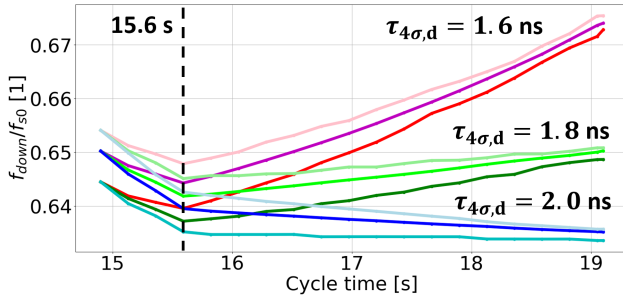


Figure 8: Minimum, mean and maximum normalized f_{down} along the blow-up time interval when $\tau_{4,d} = 1.6$ ns (red colours), 1.8 ns (green) and 2.0 ns (blue). The considered cycle is shown in Fig. 2.

diffused by phase noise as desired. As a compromise, the mean of the f_{down} values has been chosen.

The bunch distributions generated during the blow-up are binomial and, similarly to what is described above, changing μ did not significantly affect the determination of f_{down} .

The upper limit f_{up} of the frequency band was set slightly above f_{s0} (Fig. 6, orange). Indeed, for the present SPS impedance model, the synchrotron frequency distributions of the bunches are always lower than the distribution without collective effects, as shown for instance in Fig. 6, where the 72 distributions (almost superposed) are slightly below f_s .

The generic procedure described here to determine f_{down} at a given time is then repeated for a user-defined set of times during the blow-up time interval. Figure 8 shows the minimum, mean and maximum f_{down} along the cycle, when $\tau_{4,d} = 1.6$ ns, 1.8 ns and 2.0 ns. The lower f_{down} values occur when $\tau_{4,d} = 2.0$ ns, since lower synchrotron frequencies correspond to larger emittances and bunch lengths at the end of the blow-up, and therefore at extraction.

The curves in Fig. 8 change slope at 15.6 s, which is the time when the momentum ramp in Fig. 2 changes from parabolic to linear. Since the RF systems are in BSM and since the main RF voltage is constant above 14 s, this is also the time when the synchronous phase becomes constant.

MACRO-PARTICLE SIMULATIONS

Macro-particle simulations of the SPS cycle shown in Fig. 2 started at 10.6 s with 72 rotated PS bunches and ended at extraction. Simulations included collective effects,

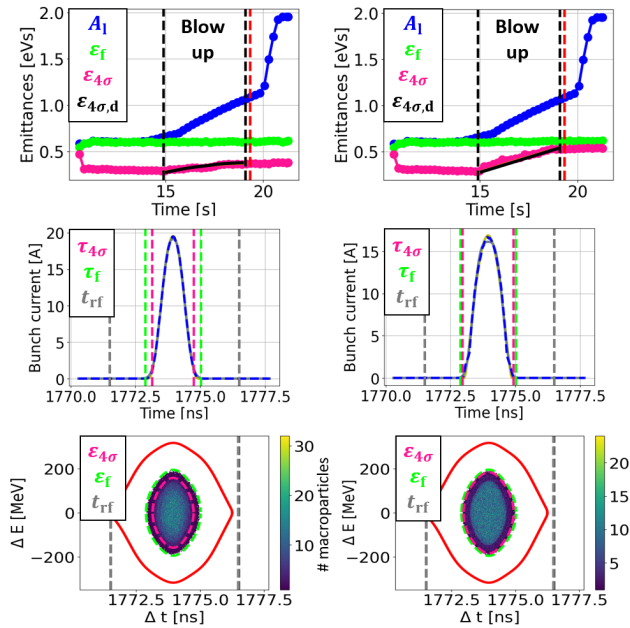


Figure 9: Simulated emittance evolutions (top), profiles at extraction (middle) and corresponding distributions in phase space (bottom) for the bunch 72 when $\tau_{4,d} = 1.6$ ns (left) and $\tau_{4,d} = 2.0$ ns (right). The blue and black curves (top) represent respectively the acceptance and design-emittance evolutions, the vertical red lines (top) mark the momentum of 380 GeV/c. The full and 4σ emittances/bunch lengths are in green and pink, respectively.

beam loops and emittance blow-up. The algorithm described above has been executed to obtain the frequency bands for desired extracted bunch lengths of 1.6 ns, 1.8 ns and 2.0 ns.

Figure 9 shows the emittance evolutions, profiles at extractions and corresponding distributions of the last bunch, when $\tau_{4,d} = 1.6$ ns and $\tau_{4,d} = 2.0$ ns. For each simulation, the phase-noise rms σ_n was kept constant during the blow-up. We found that $\sigma_n = 5$ mrad and $\sigma_n = 14$ mrad were the optimal values for $\tau_{4,d} = 1.6$ ns and $\tau_{4,d} = 2.0$ ns, respectively. Using these phase noise amplitudes, the evolution of ϵ_4 followed the design $\epsilon_{4,d}$ curves (Fig. 9, top) very well. As desired, the full emittances remained constant along the cycle, indicating that phase noise targets just the bunch core. This allows to have a loss free blow-up.

Figure 9 also shows that the extracted distributions and profiles of the last bunch do not present any structure which could degrade the quality of the extracted beam. We just observe that, when $\tau_{4,d} = 2.0$ ns, the bunch distribution has a low density stripe in the outer part, and the bunch profile is almost parabolic, with the exception of the tails. This indicates that the bunch core could be targeted even more, and indeed $\sigma_n = 20$ mrad would remove the low density stripe in the bunch distribution, although the extracted bunch length would be slightly larger than the desired one.

The observations done here for the last bunch remain valid also for the other bunches. In particular, no bunch showed any sign of quality degradation at extraction. As expected,

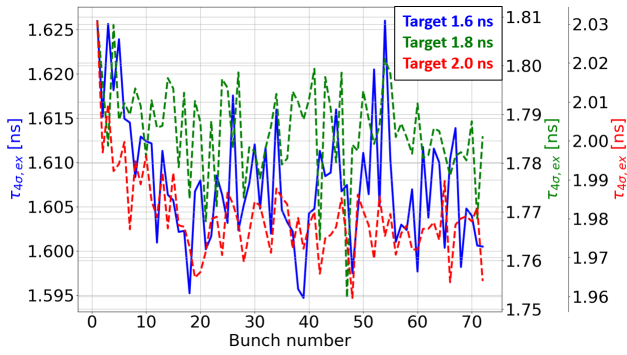


Figure 10: Simulated extracted bunch lengths along the batch when $\tau_{4,d} = 1.6$ ns (blue), 1.8 ns (green), 2.0 ns (red). The extracted profile and distribution of the last bunch when $\tau_{4,d} = 1.6$ ns and 2.0 ns are shown in Fig. 9.

the $\tau_{4,ex}$ values differed along the batch. These spreads should remain small, mostly for HL-LHC beams. Figure 10 shows that $\tau_{4,ex} = 1.61 \pm 0.02$ ns, 1.79 ± 0.04 ns, 1.98 ± 0.05 ns when $\tau_{4,d} = 1.6$ ns, 1.8 ns and 2.0 ns, respectively. The maximum spread is 4%, which would be satisfying if found also at the intensity of HL-LHC beams.

COMPARISON TO BEAM MEASUREMENTS

Simulations were compared with first beam measurements of one batch of 72 bunches accelerated either without or with emittance blow-up. When phase noise was included, we set $f_{down} = 0.64f_{s0}$ ratio during the blow-up. Although this setting was an approximation of the results shown in Fig. 8, the goal was to verify that a constant f_{down}/f_{s0} can still provide stable beams and the desired $\tau_{4,d} = 1.65$ ns during measurements. A constant f_{down}/f_{s0} would greatly simplify the phase noise setup in operation.

Figure 11 shows the minimum, mean and maximum bunch lengths along the batch as a function of the cycle time, in simulations and measurements. Without emittance blow-up (Fig. 11, top), the bunch lengths are slightly lower in simulations than in measurements, mostly for cycle times above 14 s. At flat-top, the bunch lengths are 1.57 ± 0.09 ns and 1.49 ± 0.08 ns in measurements and simulations, respectively.

When phase noise is applied (Fig. 11, bottom), the agreements in bunch lengths between measurements and simulations are better, both during the cycle and at flat-top. The final bunch lengths are 1.65 ± 0.12 ns and 1.65 ± 0.07 ns in measurements and simulations, respectively.

Although more studies are needed to explain the discrepancies without phase noise, which can be due to other noise sources present in the SPS, these first comparisons between measurements and simulations show that emittance blow-up works as desired, even with a constant normalized f_{down} .

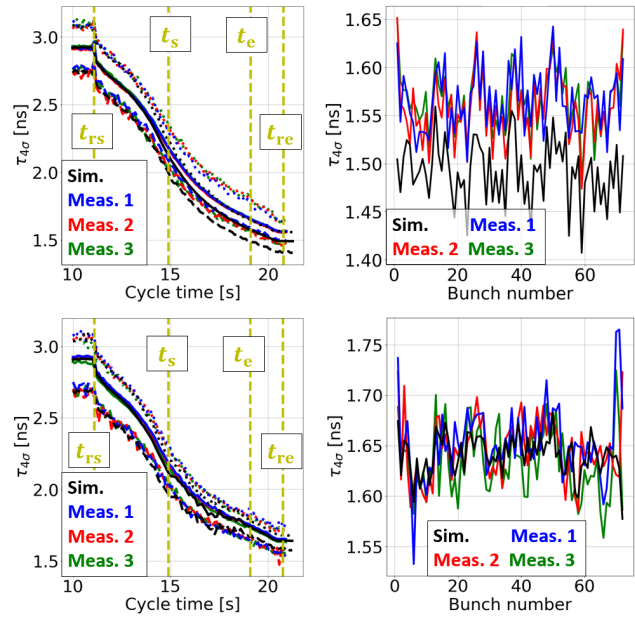


Figure 11: Left: minimum (dashed lines), mean (continuous) and maximum (dotted) bunch lengths along the cycle in simulations (black) and measurements (other colours), without (top) and with (bottom) applying phase noise between t_s and t_e . The ramp starts at t_{rs} and ends at t_{re} . Right: the corresponding final bunch lengths along the batch.

CONCLUSIONS

Controlled longitudinal emittance blow-up with bandwidth-limited phase noise is one of the major ingredients to guarantee the longitudinal stability of proton beams for the HL-LHC in the SPS.

In this paper we described an algorithm for the determination of the phase-noise frequency band. This algorithm computes the design emittance evolutions for each bunch during blow-up and determines the frequency bands using the synchrotron frequency distributions with collective effects. We showed that the optimal frequency band can change significantly according to the desired extracted bunch length.

The computed frequency bands were used in realistic macro-particle simulations of one batch of 72 bunches through the SPS cycle. It was possible to obtain different desired bunch lengths at extraction, as well as high quality extracted distributions and bunch profiles.

Results from simulations were compared with beam measurements. We found slight disagreements in bunch length when phase noise was not applied. With a proper choice of the phase noise amplitude, it was possible to obtain good agreements in bunch length when emittance blow-up was present. We showed that an approximation of the optimal frequency band can still provide the desired bunch lengths at extraction, both in measurements and simulations.

ACKNOWLEDGEMENTS

We thank B. Bielawski who developed the interfaces for an efficient use of the noise algorithm in measurements and

simulations. The simulated PS bunches were kindly provided by A. Lasheen. We also thank the SPS operation team who provided precious support during beam measurements.

REFERENCES

- [1] E. N. Shaposhnikova *et al.*, “Removing Known SPS Intensity Limitations for High Luminosity LHC Goals”, in *Proc. 7th Int. Particle Accelerator Conf. (IPAC’16)*, Busan, Korea, May 2016, pp. 989–991. doi:10.18429/JACoW-IPAC2016-MOPOY058
- [2] J. Repond, “Possible Mitigations of Longitudinal Intensity Limitations for HL-LHC Beam in the CERN SPS”, Ph.D. thesis, LPAP, EPFL, Lausanne, France, 2019.
- [3] J. Repond, M. Schwarz, and E. Shaposhnikova, “Mitigation of intensity limitation in the CERN SPS using a double RF system,” *International Journal of Modern Physics A*, vol. 34, p. 1942036, 2019. doi:10.1142/S0217751X19420363
- [4] T. Bohl, T. Linnecar, E. Shaposhnikova, and J. Tueckmantel, “Study of Different Operating Modes of the 4th RF Harmonic Landau Damping System in the CERN SPS”, in *Proc. 6th European Particle Accelerator Conf. (EPAC’98)*, Stockholm, Sweden, Jun. 1998, paper THP09A, p. 978.
- [5] T. Toyama, “Uniform bunch formation by RF voltage modulation with a band-limited white signal,” *Nuclear Instruments and Methods in Physics Research Section A: Accelerators, Spectrometers, Detectors and Associated Equipment*, vol. 447, no. 3, p. 317, 2000. doi:10.1016/S0168-9002(99)01312-1
- [6] G. Papotti *et al.*, “Study of Controlled Longitudinal Emittance Blow-up for High Intensity LHC Beams in the CERN SPS,” *Conf. Proc. C*, vol. 0806233, p. 1676, 2008.
- [7] S. Albright and D. Quartullo, “Time varying RF phase noise for longitudinal emittance blow-up,” *J. Phys.: Conf. Ser.*, vol. 1350, p. 012144, 2019. doi:10.1088/1742-6596/1350/1/012144
- [8] D. Quartullo, E. Shaposhnikova, and H. Timko, “Controlled longitudinal emittance blow-up using band-limited phase noise in CERN PSB,” *J. Phys.: Conf. Ser.*, vol. 874, p. 012066, 2017. doi:10.1088/1742-6596/874/1/012066
- [9] P. Baudreghien and T. Mastoridis, “Longitudinal emittance blow-up in the large hadron collider,” *Nuclear Instruments and Methods in Physics Research Section A: Accelerators, Spectrometers, Detectors and Associated Equipment*, vol. 726, p. 181, 2013. doi:10.1016/j.nima.2013.05.060
- [10] H. Timko, P. Baudreghien, E. N. Shaposhnikova, and T. Mastoridis, “Studies on Controlled RF Noise for the LHC”, in *Proc. 54th ICFA Advanced Beam Dynamics Workshop on High-Intensity and High-Brightness Hadron Beams (HB’14)*, East Lansing, MI, USA, Nov. 2014, paper THO4LR03, pp. 414–418.
- [11] K. Hanke *et al.*, “The LHC Injectors Upgrade (LIU) Project at CERN: Proton Injector Chain”, in *Proc. 8th Int. Particle Accelerator Conf. (IPAC’17)*, Copenhagen, Denmark, May 2017, pp. 3335–3338. doi:10.18429/JACoW-IPAC2017-WEPVA036
- [12] G. Hagemann *et al.*, “The CERN SPS Low Level RF upgrade Project”, in *Proc. 10th Int. Particle Accelerator Conf. (IPAC’19)*, Melbourne, Australia, May 2019, pp. 4005–4008. doi:10.18429/JACoW-IPAC2019-THPRB082
- [13] J. T. ckmantel, “Digital Generation of Noise-Signals with Arbitrary Constant or Time-Varying Spectra (A noise generation software package and its application),” Tech. Rep. LHC-PROJECT-Report-1055, CERN, Geneva, 2008.
- [14] “CERN BLoND Code.” <http://blond.web.cern.ch/>.